

Discrete-Time Modeling of PMSM for Parametric Estimation and Model Predictive Control Tasks

1st Lukas Zezula

CEITEC, Department of Control and Instrumentation
Brno University of Technology
Brno, Czech Republic
lukas.zezula@ceitec.vutbr.cz

2nd Petr Blaha

Central European Institute of Technology (CEITEC)
Brno University of Technology
Brno, Czech Republic
petr.blaha@ceitec.vutbr.cz

Abstract—This paper presents novel implicit and explicit discrete-time permanent magnet synchronous motor models. Both derived models solve the problem of numerical instability and poor precision of motor currents’ discrete-time prototypes formed using the forward Euler method and preserve the tolerable complexity of resulting descriptions. Discrete-time models of currents are derived based on the linear time-varying systems approach, considering the electrical angular velocity time-varying parameter. Angular velocity and angle are discretized by using the linear multistep methods. The implicit variant of the model is dedicated to parametric estimation tasks, and the explicit variant is to model predictive control. The derived descriptions are validated within the simulation by comparing the original continuous-time model and Euler approximation with the explicit model. Furthermore, the prediction capabilities of the explicit model and Euler approximation are compared as well.

Index Terms—discrete-time systems, mathematical models, model checking, parameter estimation, permanent magnet motors, predictive control, predictive models, systems modeling.

I. INTRODUCTION

Due to their reliable construction, high efficiency, and power density, permanent magnet synchronous machines (PMSMs) are commonly used in robotics, industrial drives, and vehicular propulsions. Because of its reliable operation and relatively easy implementation, numerous PMSM applications rely on field-oriented (vector) control. The linear control methods, however, can not guarantee sufficiently high performance of the PMSM drive system due to the existence of nonlinearities. In recent years, model predictive control (MPC) has been considered a promising alternative for controlling power converters and drives [1] - [3].

In general, MPC utilizes the discrete-time model of PMSM to predict a controlled system’s states. The information about expected states is then reflected in a cost function, and the desired control actions are obtained by minimizing this cost function. Therefore, the performance of MPC is highly influenced by the quality of the prediction model. Currently, authors primarily utilize the discrete-time model derived from the continuous-time description by the forward Euler method. This method provides satisfactory results only if the rate of change of approximated state variable is neglectable in the sampling period. However, the rates of change of PMSM’s currents depend on the electrical angular velocity that can grow significantly, eventually leading to the poor precision of Euler

approximation and numerical instability at higher velocities. This problem can be partially solved by utilizing higher terms of Taylor series expansion [4] or applying multistep discretization techniques [5]. However, these solutions lead to complex discrete-time descriptions compared to the Euler approximation.

Other approaches that require a sufficiently precise discrete-time model of PMSM are related to adaptive control and online parametric estimation. In recursive parametric estimation, parameters of the discrete-time models are adjusted to achieve a minimum difference between the model’s outputs and measured waveforms, for example, in terms of the least squares. Since models are compared with obtained data and no predictions are evaluated, unlike in MPC, implicit models can be utilized for parametric estimation. In this area, however, authors still primarily utilize the discrete-time model derived by the forward Euler method [6] or steady-state models [7] - [8] that are not valid during the transients. Since both these descriptions have limited use, novel discrete-time prototypes are needed. Discrete-time models are then applicable even in fault diagnostics [9], where the model-based principles commonly require the knowledge of healthy motor behavior.

The paper is organized as follows. The implicit description is derived in Section II, and its explicit variant is formed in Section III. Section IV then provides the stability analysis of traditionally used Euler approximation and derived explicit model. Section V validates the derived explicit model by comparing its outputs with the original continuous-time prototype and Euler approximation within the simulation.

II. IMPLICIT DISCRETE-TIME MODEL

The continuous-time rotor reference frame model of PMSM can be described as in

$$\frac{d}{dt} \begin{bmatrix} \lambda_d(t) \\ \lambda_q(t) \end{bmatrix} = \underbrace{\begin{bmatrix} -\frac{R_s}{L_d} & \omega_e(t) \\ -\omega_e(t) & -\frac{R_s}{L_q} \end{bmatrix}}_{\mathbf{A}(t)} \begin{bmatrix} \lambda_d(t) \\ \lambda_q(t) \end{bmatrix} + \begin{bmatrix} u_d^*(t) \\ u_q(t) \end{bmatrix} \quad (1)$$

where

$$\begin{aligned} u_d^*(t) &= u_d(t) + \frac{R_s}{L_d} \lambda_{pm} \\ \lambda_d(t) &= L_d i_d(t) + \lambda_{pm} & \lambda_q(t) &= L_q i_q(t). \end{aligned} \quad (2)$$

In (1) and (2), $i_d(t)$ and $i_q(t)$ are the rotor reference frame ($d - q$) currents, $u_d(t)$ and $u_q(t)$ represent $d - q$ voltages, $\lambda_d(t)$ and $\lambda_q(t)$ are $d - q$ fluxes, R_s is the equivalent stator windings' resistance, L_d symbolizes the direct axis inductance, L_q denotes the quadrature axis inductance, and λ_{pm} stands for the permanent magnet flux linkage. Electrical angular velocity $\omega_e(t)$ and angle $\theta_e(t)$ are then some time-dependent functions with significantly slower dynamics than currents. However, $\theta_e(t)$ is sampled with the same sampling period T_s as stator currents. This sampling rate is crucial since $\theta_e(t)$ is utilized in the rotor reference frame transformation of currents. Electrical angular velocity is then estimated from measured angle waveform, for example, using an angle tracking observer. Note that the sampling rate designed for currents' dynamics is highly overrated for velocity, and only minor changes of this variable occur during one sampling period. Therefore, the following implicit velocity approximation is applicable:

$$\omega_e(t) \approx \bar{\omega}_e = \frac{\omega_e(k+1) + \omega_e(k)}{2} \quad kT_s \leq t < (k+1)T_s \quad (3)$$

where k is the current step of discrete-time equivalent. Due to approximation (3), even the system matrix is constant over the sampling period $\mathbf{A}(t) = \mathbf{A}(\bar{\omega}_e) = \mathbf{A}$. Voltage control actions can then be approximated using the zero-order hold as in

$$\begin{aligned} u_d(t) &= u_d(k) & kT_s \leq t < (k+1)T_s \\ u_q(t) &= u_q(k) & kT_s \leq t < (k+1)T_s. \end{aligned} \quad (4)$$

As mentioned by Tóth et al. in [10], the discrete-time equivalent of linear time-varying system (1) with the constant parameters over the sampling period ($\mathbf{A}(t) = \mathbf{A}(\bar{\omega}_e) = \mathbf{A}$ on $kT_s \leq t < (k+1)T_s$) is calculated as the discrete-time equivalent of a linear time-invariant system. We have

$$\begin{bmatrix} \lambda_d(k+1) \\ \lambda_q(k+1) \end{bmatrix} = e^{\mathbf{A}T_s} \begin{bmatrix} \lambda_d(k) \\ \lambda_q(k) \end{bmatrix} + \int_0^{T_s} e^{\mathbf{A}t} dt \begin{bmatrix} u_d^*(k) \\ u_q(k) \end{bmatrix} \quad (5)$$

where the exponential of system matrix \mathbf{A} can be calculated based on the following similarity transformation:

$$\begin{bmatrix} \lambda_d(t) \\ \lambda_q(t) \end{bmatrix} = e^{-\frac{R_s(L_d+L_q)}{2L_dL_q}t} \begin{bmatrix} \lambda_x(t) \\ \lambda_y(t) \end{bmatrix}. \quad (6)$$

Substituting (6) into (1) provides the transformed system matrix $\tilde{\mathbf{A}}$ as in

$$\tilde{\mathbf{A}} = \begin{bmatrix} \frac{R_s(L_d-L_q)}{2L_dL_q} & \bar{\omega}_e \\ -\bar{\omega}_e & -\frac{R_s(L_d-L_q)}{2L_dL_q} \end{bmatrix}. \quad (7)$$

Matrix $\tilde{\mathbf{A}}$ is in a unique form which satisfies quadratic polynomial $\tilde{\mathbf{A}}^2 = \rho \mathbf{I}$, where $\mathbf{I} = \mathbf{I}^{2 \times 2}$ is the identity matrix. Bernstein and So derived the matrix exponential for such matrices in [11]. We have

$$e^{\tilde{\mathbf{A}}T_s} = \cosh(T_s\sqrt{\rho}) \mathbf{I} + \frac{\sinh(T_s\sqrt{\rho})}{\sqrt{\rho}} \tilde{\mathbf{A}} \quad (8)$$

where

$$\rho = \beta^2 - \bar{\omega}_e^2 \quad \beta = \frac{R_s(L_d - L_q)}{2L_dL_q}. \quad (9)$$

The exponential of original system matrix \mathbf{A} can then be calculated using the similarity transformation (6) as in

$$e^{\mathbf{A}T_s} = e^{-\alpha T_s} e^{\tilde{\mathbf{A}}T_s} \quad \alpha = \frac{R_s(L_d + L_q)}{2L_dL_q}. \quad (10)$$

Since ρ takes positive and negative values, the matrix exponential is generally split into two expressions valid for particular velocity intervals. To prevent this division, the matrix exponential can be approximated by the Taylor series close to the point $\rho = \rho_0 = -\bar{\omega}_e^2$. Suppose the approximation of function $\cosh(T_s\sqrt{\rho})$ as follows:

$$\begin{aligned} f(\rho) &\approx \sum_{i=0}^n \frac{f^{(i)}(\rho_0)}{i!} (\rho - \rho_0)^i = \sum_{i=0}^n \frac{f^{(i)}(-\bar{\omega}_e^2)}{i!} \beta^{2i} \\ f(\rho_0) &= \cosh(T_s\sqrt{\rho_0}) \\ f'(\rho_0) &= \frac{T_s \sinh(T_s\sqrt{\rho_0})}{2\sqrt{\rho_0}} \\ f''(\rho_0) &= \frac{T_s^2 \cosh(T_s\sqrt{\rho_0})}{4\rho_0} - \frac{T_s \sinh(T_s\sqrt{\rho_0})}{4\rho_0\sqrt{\rho_0}} \\ f^{(i)}(\rho_0) &= \frac{d^i}{d\rho_0^i} f(\rho_0). \end{aligned} \quad (11)$$

Note that the derivatives $f^{(i)}(\rho_0)$ in (11) are weighted by higher powers of $1/\bar{\omega}_e$ and T_s , converging rapidly toward zero and can be neglected. Since $\sinh(T_s\sqrt{\rho})/\sqrt{\rho} = 2f'(\rho)/T_s$, the same thing can be observed even for the approximation of $\sinh(T_s\sqrt{\rho})/\sqrt{\rho}$. Furthermore, since the $\sqrt{-\bar{\omega}_e^2} = j|\bar{\omega}_e|$, the hyperbolic functions can be replaced by trigonometric ones. Then the approximated matrix exponential read

$$e^{\mathbf{A}T_s} \approx e^{-\alpha T_s} \left(\cos(T_s\bar{\omega}_e) \mathbf{I} + \frac{\sin(T_s\bar{\omega}_e)}{\bar{\omega}_e} \tilde{\mathbf{A}} \right) \quad (12)$$

where α is defined as in (10) and $\tilde{\mathbf{A}}$ as in (7).

The input matrix of the discrete-time equivalent of system (1) is obtained by integrating the matrix exponential with respect to time (5). We have

$$\begin{aligned} \int_0^{T_s} e^{\mathbf{A}t} dt &= \\ \int_0^{T_s} e^{-\alpha t} \cos(t\bar{\omega}_e) dt \mathbf{I} + \frac{1}{\bar{\omega}_e} \int_0^{T_s} e^{-\alpha t} \sin(t\bar{\omega}_e) dt \tilde{\mathbf{A}} &= \\ e^{-\alpha T_s} \frac{\sin(T_s\bar{\omega}_e)}{\bar{\omega}_e} \mathbf{I} - \frac{1}{\bar{\omega}_e} \int_0^{T_s} e^{-\alpha t} \sin(t\bar{\omega}_e) dt \text{adj}(\mathbf{A}) \end{aligned} \quad (13)$$

where $\text{adj}(\mathbf{A})$ is the adjugate of system matrix \mathbf{A} . The integral in (13) can then be evaluated analytically as follows:

$$\begin{aligned} I &= \int_0^{T_s} e^{-\alpha t} \sin(t\bar{\omega}_e) dt \\ I &= \frac{\bar{\omega}_e}{\alpha^2 + \bar{\omega}_e^2} - e^{-\alpha T_s} \frac{\alpha \sin(T_s\bar{\omega}_e) + \bar{\omega}_e \cos(T_s\bar{\omega}_e)}{\alpha^2 + \bar{\omega}_e^2}. \end{aligned} \quad (14)$$

However, the primitive function I contains rational expression $1/(\alpha^2 + \bar{\omega}_e^2)$, which is unhandy for parametric estimation.

Therefore, the integral is evaluated numerically by using Simpson's 1/3 rule. We have

$$I \approx \hat{I} = \frac{T_s}{6} \left(4e^{-\frac{\alpha}{2}T_s} \sin\left(T_s \frac{\bar{\omega}_e}{2}\right) + e^{-\alpha T_s} \sin(T_s \bar{\omega}_e) \right). \quad (15)$$

The intervals of α and $\bar{\omega}_e$ feasible values have to be specified to analyze the error of approximation (15). A current's loop bandwidth mostly limits the electrical angular velocity. As mentioned by Sul in [12], the maximum of this bandwidth can reach up to $2\pi/(3.5T_s)$. Hence, the velocity can be described using a scaling factor s_ω as $\bar{\omega}_e = 2\pi s_\omega/(3.5T_s)$, where $s_\omega \in \langle -1, 1 \rangle$. Parameter α then represents the average of the reciprocal values of $d - q$ time constants. The sampling period must be smaller than these time constants to correctly track $d - q$ currents' changes. The most restrictive limitation of parameter α is then given as $\alpha < 1/T_s$ leading to description $\alpha = s_\alpha/T_s$, where the scaling factor $s_\alpha \in (0, 1)$. Afterward, the percent error of the integral's approximation $\delta = 100 |(I - \hat{I})/I|$ can be expressed as a function of scaling factors $\delta = f(s_\alpha, s_\omega)$ and plotted on feasible s_α and s_ω intervals. Figure 1 visualizes the percent error of utilized approximation (15).

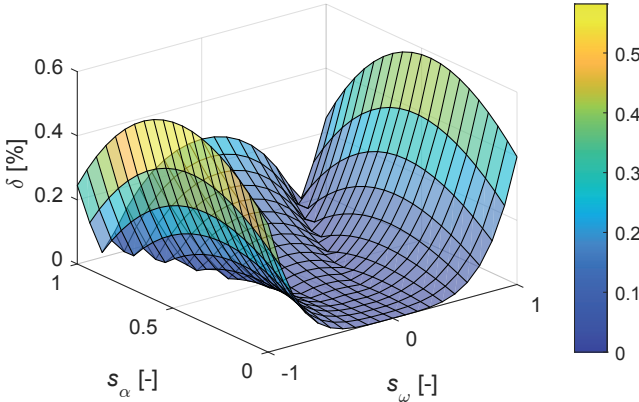


Fig. 1. Percent error of integral approximation (15)

As seen in Figure 1, the percent error of approximation (15) will not exceed 0.6 %.

The discrete-time model derived for fluxes can be expressed using currents as state variables. We have

$$\begin{bmatrix} i_d(k+1) \\ i_q(k+1) \end{bmatrix} = \mathbf{A}_d \begin{bmatrix} i_d(k) \\ i_q(k) \end{bmatrix} + \mathbf{B}_d \begin{bmatrix} u_d(k) \\ u_q(k) - \bar{\omega}_e \lambda_{pm} \end{bmatrix} \quad (16)$$

where the discrete-time state and input matrices \mathbf{A}_d and \mathbf{B}_d read

$$\mathbf{A}_d = \underbrace{\begin{bmatrix} \frac{1}{L_d} & 0 \\ 0 & \frac{1}{L_q} \end{bmatrix}}_{\mathbf{L}^{-1}} e^{\mathbf{A}T_s} \underbrace{\begin{bmatrix} L_d & 0 \\ 0 & L_q \end{bmatrix}}_{\mathbf{L}}$$

$$\mathbf{A}_d \approx e^{-\alpha T_s} \left(\cos(T_s \bar{\omega}_e) \mathbf{I} + \frac{\sin(T_s \bar{\omega}_e)}{\bar{\omega}_e} \begin{bmatrix} \beta & \frac{L_q \bar{\omega}_e}{L_d} \\ -\frac{L_d \bar{\omega}_e}{L_q} & -\beta \end{bmatrix} \right)$$

$$\mathbf{B}_d = \mathbf{L}^{-1} \int_0^{T_s} e^{\mathbf{A}t} dt$$

$$\mathbf{B}_d \approx e^{-\alpha T_s} \frac{\sin(T_s \bar{\omega}_e)}{\bar{\omega}_e} \begin{bmatrix} \frac{1}{L_d} + \frac{T_s R_s}{6 L_d L_q} & \frac{T_s \bar{\omega}_e}{6 L_d} \\ -\frac{T_s \bar{\omega}_e}{6 L_q} & \frac{1}{L_q} + \frac{T_s R_s}{6 L_d L_q} \end{bmatrix} + \frac{2}{3} T_s e^{-\frac{\alpha}{2} T_s} \frac{\sin\left(T_s \frac{\bar{\omega}_e}{2}\right)}{\bar{\omega}_e} \begin{bmatrix} \frac{R_s}{L_d L_q} & \frac{\bar{\omega}_e}{L_d} \\ \frac{\bar{\omega}_e}{L_q} & \frac{R_s}{L_d L_q} \end{bmatrix}. \quad (17)$$

In (17), parameters α and β are defined as in (10) and (9).

The following differential equations describe electrical angular velocity and angle:

$$\frac{d}{dt} \omega_e(t) = \frac{p}{J} \tau_e(t) - \frac{p}{J} \tau_l(t)$$

$$\tau_e(t) = \frac{3}{2} p (\lambda_{pm} i_q(t) + (L_d - L_q) i_d(t) i_q(t))$$

$$\frac{d}{dt} \theta_e(t) = \omega_e(t) \quad (18)$$

where p is the number of pole pairs, J stands for the moment of inertia, $\tau_e(t)$ is the electromagnetic torque of a motor, and $\tau_l(t)$ is a torque load. Since only minor $\omega_e(t)$ changes occur during the sampling period, the electrical angular velocity can be implicitly approximated by using the second-order Adams-Moulton method (trapezoidal rule) as in

$$\omega_e(k+1) = \omega_e(k) + \frac{p}{J} T_s (\bar{\tau}_e - \bar{\tau}_l)$$

$$\bar{\tau}_e = \frac{1}{2} (\tau_e(k+1) + \tau_e(k))$$

$$\bar{\tau}_l = \frac{1}{2} (\tau_l(k+1) + \tau_l(k)). \quad (19)$$

Similarly, the electrical angle reads

$$\theta_e(k+1) = \theta_e(k) + T_s \bar{\omega}_e \quad (20)$$

where the average velocity $\bar{\omega}_e$ is defined as in (3). Note that, according to expression (20), the arguments $T_s \bar{\omega}_e$ and $T_s \bar{\omega}_e/2$ of trigonometric functions in (17) can be replaced by angle differences $\theta_e(k+1) - \theta_e(k)$ and $(\theta_e(k+1) - \theta_e(k))/2$.

III. EXPLICIT DISCRETE-TIME MODEL

In the implicit discrete-time model described in Section II, the information about the angular velocity in step $k+1$ is required to calculate $d - q$ currents in step $k+1$ (a similar statement can be observed for velocity in step $k+1$ that is calculated by using $d - q$ currents in step $k+1$). The implicit formulation of the model can be utilized in parametric estimation tasks; however, for the purpose of model predictive control, the implicit model can not be used. Therefore, the discrete-time model has to be expressed in an explicit way (where state variables in step $k+1$ depend only on state variables and inputs in step k). To obtain an explicit model with the same precision as the implicit one, equations (16), (19), and (20) must be solved in terms of variables $i_d(k+1)$, $i_q(k+1)$, $\omega_e(k+1)$, and $\theta_e(k+1)$. However, the complexity of the problem would lead to unnecessarily complicated results. Therefore, to preserve the tolerable complexity of the discrete-time model, the explicit model is formed using less precise

numerical approximations. Since the rate of change of $\omega_e(t)$ and $\theta_e(t)$ is neglectable in the sampling period, the Euler approximation is used to discretize these variables. We have

$$\begin{aligned}\omega_e(k+1) &= \omega_e(k) + \frac{p}{J} T_s (\tau_e(k) - \tau_l(k)) \\ \theta_e(k+1) &= \theta_e(k) + T_s \omega_e(k).\end{aligned}\quad (21)$$

In Section II, rotor reference frame currents were discretized using the implicit velocity approximation (3). However, to obtain an explicit formulation, the angular velocity can be approximated by the value obtained at the beginning of the sampling period as follows:

$$\omega_e(t) \approx \omega_e(k) \quad kT_s \leq t < (k+1)T_s. \quad (22)$$

Then the explicit discrete-time prototype of $d-q$ currents is obtained by substituting $\omega_e(k)$ for $\bar{\omega}_e$ in (16) and (17).

IV. STABILITY ANALYSIS

One of the most remarkable contributions of the derived discrete-time models can be observed by analyzing the stability of discretized currents. First, suppose the Euler approximation of $d-q$ currents as in

$$\begin{aligned}\begin{bmatrix} i_d(k+1) \\ i_q(k+1) \end{bmatrix} &= \mathbf{A}_{d,E} \begin{bmatrix} i_d(k) \\ i_q(k) \end{bmatrix} + \mathbf{B}_{d,E} \begin{bmatrix} u_d(k) \\ u_q(k) - \omega_e(k)\lambda_{pm} \end{bmatrix} \\ \mathbf{A}_{d,E} &= \begin{bmatrix} 1 - T_s \frac{R_s}{L_d} & T_s \frac{L_q \omega_e(k)}{L_d} \\ -T_s \frac{L_d \omega_e(k)}{L_q} & 1 - T_s \frac{R_s}{L_q} \end{bmatrix} \\ \mathbf{B}_{d,E} &= \begin{bmatrix} \frac{T_s}{L_d} & 0 \\ 0 & \frac{T_s}{L_q} \end{bmatrix}.\end{aligned}\quad (23)$$

System (23) is stable if and only if the velocity-dependent eigenvalues of the system matrix $\mathbf{A}_{d,E}$ lie inside the unit circle in the complex plane. The calculated eigenvalues read

$$\zeta_{1,2}^E = (1 - \alpha T_s) \pm j T_s \sqrt{\omega_e(k)^2 - \beta^2} \quad (24)$$

where j is the imaginary unit. According to the stability condition $|\zeta_{1,2}^E| < 1$, the following velocity limitation can be derived:

$$|\omega_e(k)| < \sqrt{\frac{1}{T_s} \frac{R_s(L_d + L_q)}{L_d L_q} - \frac{R_s^2}{L_d L_q}}. \quad (25)$$

The limitation (25) is very restrictive compared to the velocity bandwidth reaching up to $2\pi/(3.5T_s)$. Hence, the discrete-time model derived by the Euler approximation is unstable for higher velocities.

The problem with instability is resolved by the discrete-time models derived in the previous sections. The eigenvalues of the explicit variant of system matrix \mathbf{A}_d (17) read

$$\zeta_{1,2} = e^{-\alpha T_s} \cos(T_s \omega_e(k)) \pm j \frac{\sqrt{\omega_e(k)^2 - \beta^2}}{\omega_e(k)} \sin(T_s \omega_e(k)) \quad (26)$$

where function $\sqrt{\omega_e(k)^2 - \beta^2}/\omega_e(k)$ does not have extremum and converges toward 1 with the growing velocity. If this limit

value is substituted for the original function, the absolute value of eigenvalues can be calculated as in

$$|\zeta_{1,2}| = \sqrt{e^{-2\alpha T_s} \cos^2(T_s \omega_e(k)) + \sin^2(T_s \omega_e(k))}. \quad (27)$$

Hence, the stability condition $|\zeta_{1,2}| < 1$ results in requirement $\alpha > 0$, and therefore the derived implicit and explicit discrete-time prototypes of $d-q$ currents are stable over the entire velocity range.

V. MODEL VALIDATION

As mentioned in Section III, the explicit model is less precise than the implicit one. Therefore, the validation is aimed at the explicit model. This model is compared with its continuous-time equivalent (1), (2), and (18) and the discrete-time model (23), and (21) obtained by the forward Euler discretization method within the MATLAB Simulink simulation. The continuous-time model is solved using the ode45 (Dormand-Prince) MATLAB variable-step solver with the maximum step size $100 \mu\text{s}$ and relative tolerance 1×10^{-6} . The discrete-time parts utilize the sampling period of $100 \mu\text{s}$. Parameters of the simulated motor are presented in the table below:

TABLE I
PARAMETERS OF THE SIMULATED MOTOR

Parameter	Value	Parameter	Value
R_s [m Ω]	6	p [-]	10
L_d [μH]	100	J [kg m ²]	0.03
L_q [μH]	200	U_{dc} [V]	400
λ_{pm} [mWb]	12	I_{max} [A]	200

where U_{dc} stands for the DC bus voltage and I_{max} describes the limitation of current vector.

In one part of the validation experiment, all the models utilize the same inputs $u_d(k)$, $u_q(k)$, and $\tau_l(k)$, and the output rotor reference frame currents and electrical angular velocity are compared. Voltage inputs are generated by the field-oriented control system that controls the velocity of the continuous-time model to the setpoint. The input waveforms are visualized in Figure 2.

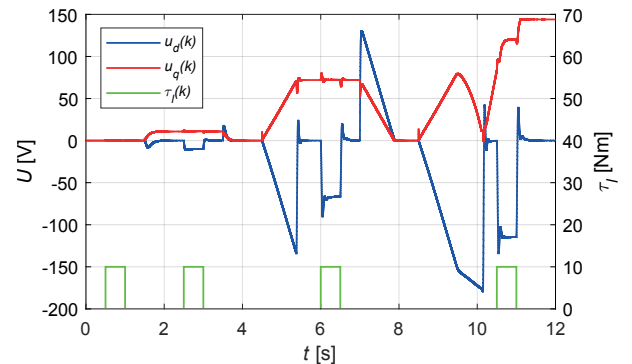


Fig. 2. Shared inputs to the discrete and continuous-time models

Figure 3 then shows the velocity responses of models to shared voltage and torque load inputs and the error of the

explicit model $\Delta\omega_e$ evaluated as the difference between the continuous-time model and the explicit one in $100 \mu\text{s}$ steps.

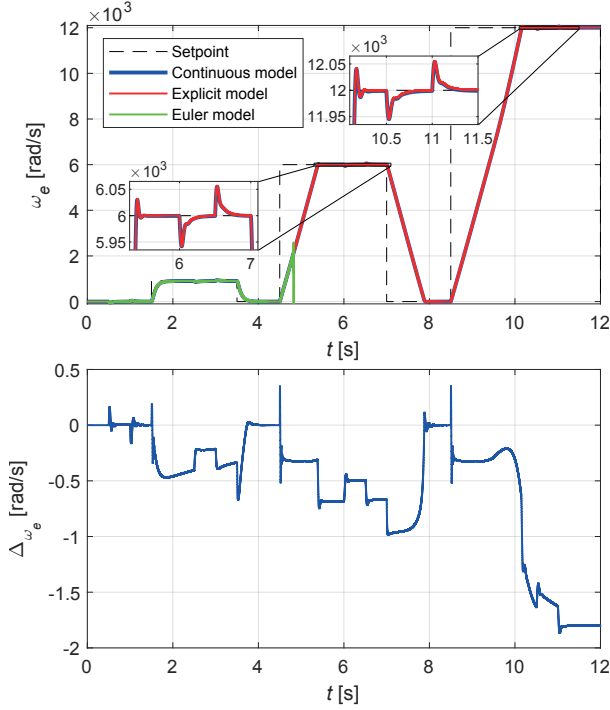


Fig. 3. Velocity responses of models and error of the explicit model

A similar comparison of $d - q$ currents responses and errors is displayed in Figure 4.

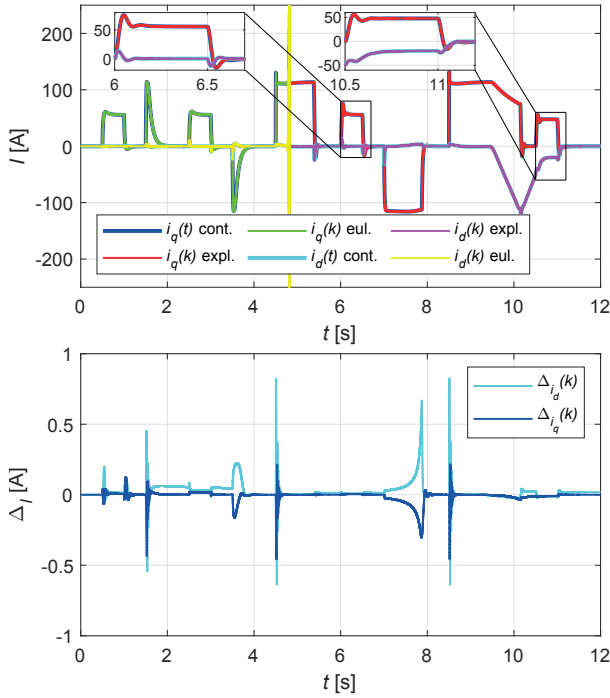


Fig. 4. Currents responses of models and errors of the explicit model

Figures 3 and 4 illustrate that the forward Euler method-based model exhibits instability at relatively low angular velocities compared to the entire motor's bandwidth. Since the model

is tested in the open loop using voltages generated for the stable continuous-time description, its numerical instability remains unaddressed. Including the closed-loop control in the comparison could partially address the instability, but voltage errors arise. On the other hand, the explicit model tracks the continuous responses even on high angular velocities, and its errors of velocity and currents are mostly neglectable relative to the velocity value and the current's vector amplitude.

In the other part of the validation experiment, the prediction capabilities of the explicit model and Euler approximation are compared. The simulated motor is driven to the angular velocity setpoint, and in time 2.5 s, the torque load step of 10 Nm is realized. Discrete-time models are then utilized to predict the value of currents, voltages, and velocity after 10 steps of the closed-loop system. Predicted values are compared with the results calculated using the continuous-time prototype, and the error of the explicit and Euler models are evaluated. Comparisons of predicted voltages, currents, and velocities by different models are visualized together with errors in Figures 5, 6, and 7. As seen in these figures, the errors of the Euler model are much more significant than that of the explicit model, especially in areas where rapid variable change occurs. Predictions of velocities are mostly comparable since both models utilize the same discrete-time velocity prototype.

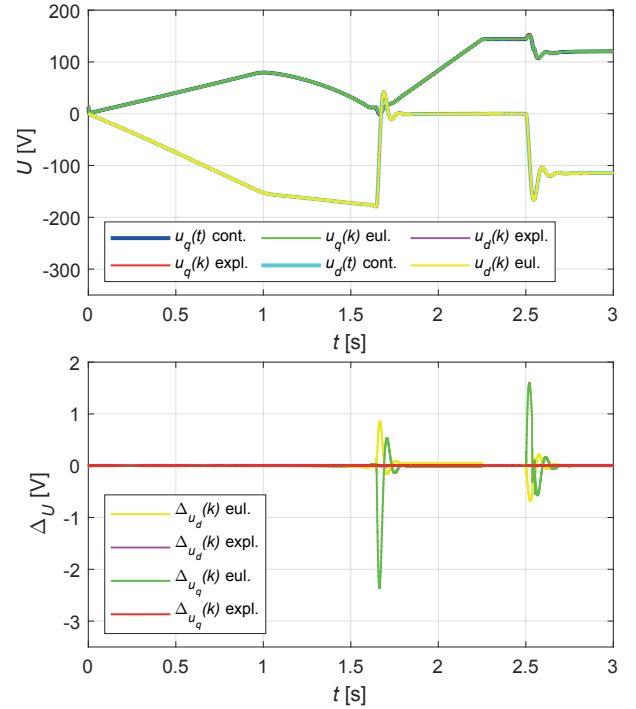


Fig. 5. Voltages predicted in 10 steps horizon and prediction errors

Updating the forward Euler method-based model requires approximately 9 parameters, 11 multiplications (\times), and 8 summations ($+$), while the update of the explicit model requires about 16 parameters, 26 \times , 16 $+$, and evaluation of functions $\cos(x)$, $\text{sinc}(x)$, and $\text{sinc}(x/2)$, which can be replaced (assuming only the feasible values of $\bar{\omega}_e$) by their fourth-order Taylor series, necessitating 9 \times , and 6 $+$.

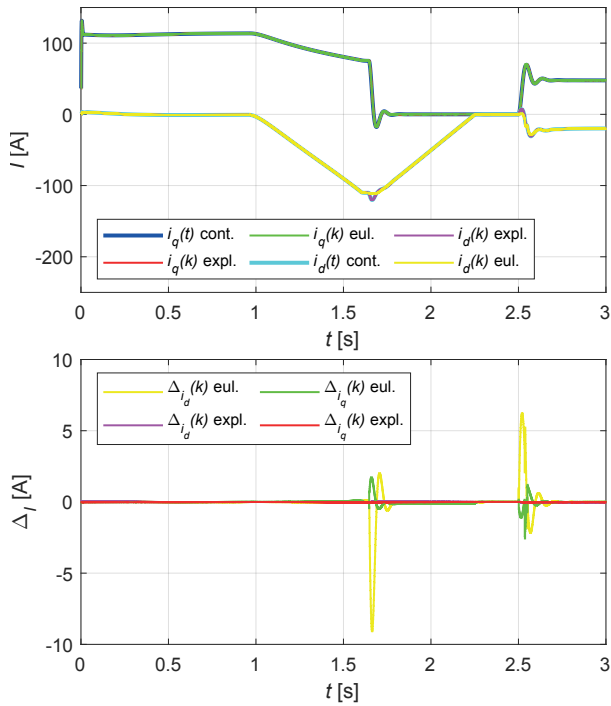


Fig. 6. Currents predicted in 10 steps horizon and prediction errors

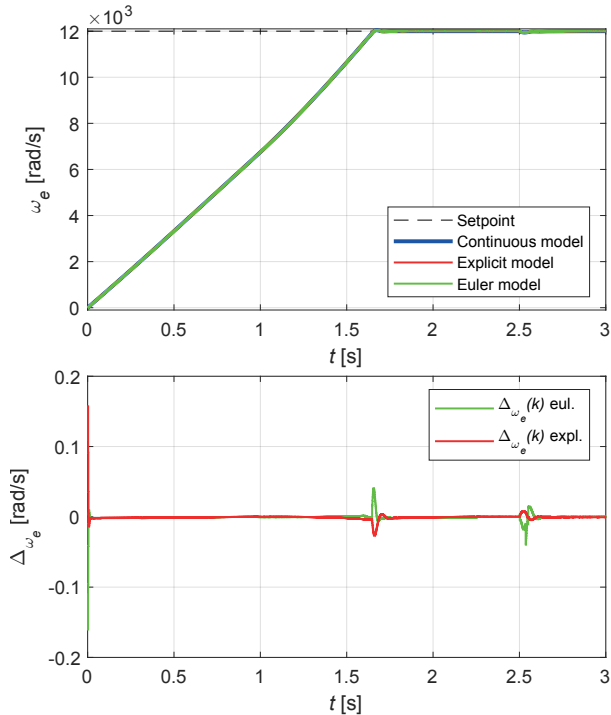


Fig. 7. Velocities predicted in 10 steps horizon and prediction errors

VI. CONCLUSION

In this paper, the discrete-time modeling of PMSM was discussed, and two models were derived. The more precise implicit discrete-time model is dedicated to parametric estimation tasks, and the explicit model is then to model predictive control. Both these models solve the problems of poor precision and instability of the commonly used forward Euler method-based model and preserve tolerable complexity.

VII. ACKNOWLEDGMENT

The first author has been supported by the Czech Science Foundation under the project 23-06476S: Analysis of Discrete and Continuous Dynamical Systems with Emphasis on Identification Problems. The work of the second author has been performed in the project AI4CSM: Automotive Intelligence for/at Connected Shared Mobility No 101007326/8A21013 and was co-funded by grants of the Ministry of Education, Youth and Sports of the Czech Republic and Electronic Component Systems for European Leadership Joint Undertaking (ECSEL JU). Their work was also supported by the infrastructure of RICAIP that has received funding from the European Union's Horizon 2020 research and innovation programme under grant agreement No 857306 and from Ministry of Education, Youth and Sports under OP RDE grant agreement No CZ.02.1.01/0.0/0.0/17_043/0010085. L. Zezula is the Brno Ph.D. Talent Scholarship Holder funded by the Brno City Municipality.

REFERENCES

- [1] S. Vazquez, J. Rodriguez, M. Rivera, L. G. Franquelo and M. Norambuena, "Model Predictive Control for Power Converters and Drives: Advances and Trends," in *IEEE Trans. Ind. Electron.*, vol. 64, no. 2, pp. 935-947, Feb. 2017, doi: 10.1109/TIE.2016.2625238.
- [2] D. F. Valencia, R. Tarviridilu-Asl, C. Garcia, J. Rodriguez and A. Emadi, "Vision, Challenges, and Future Trends of Model Predictive Control in Switched Reluctance Motor Drives," in *IEEE Access*, vol. 9, pp. 69926-69937, 2021, doi: 10.1109/ACCESS.2021.3078366.
- [3] H. Liu and S. Li, "Speed Control for PMSM Servo System Using Predictive Functional Control and Extended State Observer," in *IEEE Trans. Ind. Electron.*, vol. 59, no. 2, pp. 1171-1183, Feb. 2012, doi: 10.1109/TIE.2011.2162217.
- [4] P. Vaclavek and P. Blaha, "PMSM model discretization for Model Predictive Control algorithms," *Proceedings of the 2013 IEEE/SICE International Symposium on System Integration*, 2013, pp. 13-18, doi: 10.1109/SII.2013.6776649.
- [5] M. Kögel and R. Findeisen, "Discrete-time robust model predictive control for continuous-time nonlinear systems," 2015 *Am. Control Conf. (ACC)*, Chicago, IL, USA, 2015, pp. 924-930, doi: 10.1109/ACC.2015.7170852.
- [6] D. Friml, M. Kozubík and P. Václavek, "On Improving TLS Identification Results Using Nuisance Variables with Application on PMSM," *IECON 2021 – 47th Annual Conference of the IEEE Industrial Electronics Society*, Toronto, ON, Canada, 2021, pp. 1-6, doi: 10.1109/IECON48115.2021.9589402.
- [7] K. Liu, Q. Zhang, J. Chen, Z. Q. Zhu and J. Zhang, "Online Multiparameter Estimation of Nonsalient-Pole PM Synchronous Machines With Temperature Variation Tracking," in *IEEE Trans. Ind. Electron.*, vol. 58, no. 5, pp. 1776-1788, May 2011, doi: 10.1109/TIE.2010.2054055.
- [8] S. J. Underwood and I. Husain, "Online Parameter Estimation and Adaptive Control of Permanent-Magnet Synchronous Machines," in *IEEE Trans. Ind. Electron.*, vol. 57, no. 7, pp. 2435-2443, July 2010, doi: 10.1109/TIE.2009.2036029.
- [9] T. Orłowska-Kowalska et al., "Fault Diagnosis and Fault-Tolerant Control of PMSM Drives—State of the Art and Future Challenges," in *IEEE Access*, vol. 10, pp. 59979-60024, 2022, doi: 10.1109/ACCESS.2022.3180153.
- [10] R. Tóth, P. M. J. Van den Hof, and P. S. C. Heuberger, "Discretisation of linear parameter-varying state-space representations," *IET Control Theory & Applications*, vol. 4, no. 10, Institution of Engineering and Technology (IET), pp. 2082–2096, Oct. 01, 2010, doi: 10.1049/iet-cta.2009.0572.
- [11] D. S. Bernstein and W. So, "Some explicit formulas for the matrix exponential," in *IEEE Trans. Autom. Control*, vol. 38, no. 8, pp. 1228-1232, Aug. 1993, doi: 10.1109/9.233156.
- [12] S. K. Sul, *Control of electric machine drive system*. Hoboken, N.J.: Wiley-IEEE Press, 2011. ISBN 978-0-470-59079-9.